Pseudogaps and the spin-bag approach to high-T_c superconductivity

A. Kampf* and J. R. Schrieffer†
Advanced Studies Program in High Temperature Superconductivity Theory, Los Alamos National Laboratory, Los Alamos, New Mexico 87545
(Received 2 October 1989)

It is shown that antiferromagnetic spin fluctuations in a two-dimensional metal, such as heavily doped cuprate superconductors, lead to a pseudogap in the electronic spectrum. The spectral function evolves from one peak in the Fermi-liquid regime to two peaks, one for particles and one for holes. The self-energy of spin bags and their pairing interaction are calculated. These results are consistent with the corresponding results in the weakly doped ordered antiferromagnet.

I. INTRODUCTION

High-temperature oxide superconductors exhibit antiferromagnetism and superconductivity in nearby regions of the phase diagram, as shown schematically in Fig. 1, where x denotes the doping concentration. Recent experiments show that the qualitative features of the phase diagram are the same for either hole or electron doping,[1] suggesting that particle-hole symmetric models are favored. Furthermore, neutron[2] and Raman[3] scattering experiments have established in the superconducting phase, the existence of antiferromagnetic spin correlations whose range is large compared with the lattice spacing. It is plausible that the existence of high-T_c superconductivity is intimately related to these spin correlations.

In developing a theoretical understanding of these phenomena, two limiting points of view have been taken. The first, advanced by Anderson,[4] assumes that the on-site effective electron-electron Coulomb repulsion U is large compared to the bandwidth W. In this approach one starts from the Mott Hubbard insulating state in which all sites are singly occupied. While this state is antiferromagnetic, it is presumed that for doping beyond a critical concentration the system enters a phase in which pairs of spins are coupled to total spin zero, with these pair bonds resonating over all possible spin configurations. Excitations in this scheme are assumed to carry charge e and spin 0 (holons) or charge zero and spin $\frac{1}{2}$ (spinons). This resonating-valence-bond (RVB) approach leads to superconductivity only when interplanar electron hopping is taken into account.

In related work, a number of authors have explored the existence of neutral spin-$\frac{1}{2}$ excitations in frustrated antiferromagnets. Wen, Wilczek, and Zee[5] have shown that a parity- and time-reversal-violating spin-order parameter of the form $\mathbf{S}_1\cdot(\mathbf{S}_2\times\mathbf{S}_3)$ can exist if the frustration is of the proper form. Laughlin[6] has proposed that in such frustrated antiferromagnets, quasiparticles exhibiting fractional statistics can lead to superconductivity. In addition there are several informative studies[7] of the dynamics of one or more holes hopping in a Heisenberg antiferromagnet having long range order. Thus, large-U models exhibit a rich set of phenomena. Whether these include a valid theory of high-temperature superconductivity in cuprates is unclear at present.

The other limiting point of view is that U is smaller than the bandwidth W. In this case the electrons are taken to zero order as being itinerant, with antiferromagnetism described as a spin-density wave (SDW). If the Fermi surface has appropriate nesting properties, as in the half-filled two-dimensional square lattice with nearest-neighbor hopping, a gap Δ_{SDW} extends over the entire Fermi surface and the system is an antiferromagnetic insulator, as in the large-U Hubbard model. The quasiparticles in the SDW phase carry charge e ($-e$) and spin $\frac{1}{2}$ as conventional holes and electrons. However, a quasiparticle alters the sublattice magnetization in its vicinity and forms a region of reduced antiferromagnetic order termed a spin bag extending over a distance equal to the SDW coherence length, $\xi=\hbar v_F/\Delta_{\mathrm{SDW}}$ (Ref. 8), which moves with the particle.

As Wen, Zhang, and one of the present authors (SWZ) (Ref. 9) have shown, the pairing interaction between two of these spin bags is attractive at small momentum transfer, reflecting the reduced exchange gap inside the SDW coherence volume surrounding each excitation. Within the pairing theory, one finds that the doped material exhibits superconductivity with a gap Δ_{SC} which is nodeless over the entire hole (electron) Fermi surface.

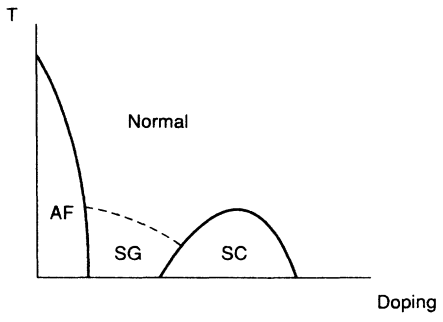

FIG. 1. A schematic phase diagram of the cuprate superconductors. AF, antiferromagnetic; SG, spin glass; SC, superconducting. x is the hole concentration.

Therefore, the temperature dependence of quantities such as the NMR relaxation and acoustic attenuation rates, surface resistance, penetration depth, etc. are expected to be activated at low temperatures, as in conventional s-wave superconductors. We note that the pairing attraction in this approach basically arises from the dynamics of the holes and spin degrees of freedom in the two-dimensional layers, in contrast with the resonating-valence-bond (RVB) approach which relies on interplanar coupling. In the spin-bag approach, three-dimensional superconductivity in these layered materials results from holes hopping between planes coupling the phases of the finite-range pairing correlations, already well developed in the planes into a coherent three-dimensional state.

While the SWZ analysis is carried out in the antiferromagnetic phase, for which spin-up and spin-down holes tend to live on different sublattices, they argue that the resulting pairing interaction is insensitive to the presence of long-range spin order so long as the spin-spin correlation length L_{SS} is large compared to the in-plane superconducting coherence length $\xi_{SC}=\hbar v_F/\pi\Delta_{SC}$. Experimentally, it appears that these quantities are comparable for many high-temperature superconductors, although there remains considerable uncertainty about both quantities for most materials.

In the present paper, we approach the problem from the paramagnetic metal phase (large x) rather than the antiferromagnetic (AF) phase (small x). First, the one particle self-energy is studied for a model form of the dynamic spin susceptibility, $\chi(\mathbf{q},\omega)$. The familiar mass renormalization of Fermi liquid theory is obtained if χ varies smoothly on the scale of the Fermi momentum and the Fermi energy, appropriate to U small compared to W. For suitable nesting properties, as U increases χ becomes peaked as a function of $\mathbf{q}$ in the vicinity of the nesting wave vector $\mathbf{Q}$ and its characteristic frequency is reduced from the Fermi energy to the spin-fluctuation energy. In this regime, the one-particle spectral weight begins to develop two new quasiparticle peaks, rather than the one peak of conventional Fermi liquid theory whose weight vanishes as AF order sets in. One finds that the density of states smoothly evolves from a modest renormalization at the Fermi surface for small U to a suppression when strong antiferromagnetic fluctuations build up. As long-range spin order sets in, the pseudogap becomes the SDW gap.

While the model susceptibility calculations illustrate the physics of the problem, to obtain a more quantitative understanding of the pseudogap formation we have carried out detailed numerical calculations of the susceptibility within a random-phase approximation (RPA), as a function of U and doping level x. These results are consistent with the model studies mentioned above and show the smooth evolution of Fermi liquid to pseudogap behavior.

The pairing interaction arising from the local suppression of antiferromagnetic fluctuations is then calculated using the model forms of χ. While the conventional one-antiparamagnon exchange leads to a repulsive interaction, it is readily seen that the existence of the pseudogap provides a qualitatively new mechanism for the pairing attraction in the paramagnetic metal (PM) phase[8] just as SWZ (Ref. 9) deduced in the AF phase. In the PM phase, the leading-order pairing interaction is represented by a diagram consisting of two crossed spin fluctuations lines. The physical meaning of this diagram is discussed and the results are compared with those obtained in the AF phase.

II. MODEL SUSCEPTIBILITY

We consider the 2D single-orbital Hubbard model on a square lattice

$$H=-t\sum_{\langle ij\rangle\sigma}(C_{i\sigma}^{\dagger}C_{j\sigma}+C_{j\sigma}^{\dagger}C_{i\sigma})+U\sum_i n_{i\uparrow}n_{i\downarrow}-\mu\sum_{i\sigma}n_{i\sigma}\ , \tag{1}$$

where $C_{i\sigma}^{\dagger}$ and $C_{i\sigma}$ are creation and annihilation operators for localized electron states of spin σ on site i, and $n_{i\sigma}=C_{i\sigma}^{\dagger}C_{i\sigma}$. μ is the chemical potential. It is well known that with increasing Coulomb repulsion U, the Hubbard model develops strong antiferromagnetic correlations between spins on nearest-neighbor sites. At precisely half-filling, the nesting property of the Fermi surface of the tight-binding band

$$\varepsilon_k=-2t(\cos k_x a+\cos k_y a) \tag{2}$$

gives rise to a ground-state instability leading to a spin-density wave. This becomes most evident in the strong-coupling limit $U/t\gg 1$, where to leading order in t/U the Hubbard model is approximately equivalent to an antiferromagnetic (AF) spin-$\frac{1}{2}$ Heisenberg model.[10] The 2D spin-$\frac{1}{2}$ Heisenberg model itself establishes long-range AF order at zero temperature.[11] Away from half-filling $\mu<0$ or at finite temperature, antiferromagnetic correlations persist giving rise to a finite spin-spin correlation length, L_{SS}.

In a RPA treatment of the longitudinal spin-density correlation function, the instability to an SDW is determined by the Stoner criterion

$$1=U\chi_0(\mathbf{q},\omega=0)\ . \tag{3}$$

$\chi_0(\mathbf{q},\omega)$ is the correlation function in the absence of the interaction and is given by

$$\chi_0(\mathbf{q},\omega)=\frac{1}{N}\sum_{\mathbf{k}}\left[-\frac{n_{\mathbf{k}}(1-n_{\mathbf{k}+\mathbf{q}})}{\omega+\varepsilon_{\mathbf{k}}-\varepsilon_{\mathbf{k}+\mathbf{q}}-i\delta}+\frac{n_{\mathbf{k}+\mathbf{q}}(1-n_{\mathbf{k}})}{\omega+\varepsilon_{\mathbf{k}}-\varepsilon_{\mathbf{k}+\mathbf{q}}+i\delta}\right] \tag{4}$$

with the electron occupation number $n_{\mathbf{k}}$. At half-filling ($\mu=0$) $\chi_0(\mathbf{q},\omega=0)$ has a strong logarithmic divergence $\sim\ln^2 T$ (Ref. 12) at the nesting wave vectors $\mathbf{Q}=(\pm\pi,\pm\pi)$, i.e., the four corners of the first Brillouin zone, and the Stoner criterion can be satisfied for a finite value of U at a finite temperature. Away from half-filling ($\mu\neq 0$), the spin susceptibility $\chi_0(\mathbf{q},\omega=0)$ develops a maximum either at or close to $\mathbf{q}=\mathbf{Q}$, with the Stoner criterion determining a threshold value U_C for the formation of an SDW, which can be commensurate or incom-

mensurate depending on temperature and band filling.[13]

In the presence of a spin-density wave with long-range order a gap opens up in the single particle excitation spectrum. In weak coupling $U < t$ the gap Δ_{SDW} is exponentially small, while in strong coupling Δ_{SDW} is of order U (Ref. 9). In the paramagnetic metal regime, finite-range spin correlations cause the density of states to show a depletion of spectral weight near the Fermi level, reflecting the nearby instability to antiferromagnetic ordering. The formation of this pseudogap may be viewed as a precursor effect to the metal-insulator transition. The situation is similar for the $BaPb_xBi_{1-x}0_3$ compounds where the instability arises from the formation of a charge-density wave rather than a spin-density wave[14] (SDW) (see Fig. 2).

For a finite-hole concentration we study the effects of spin fluctuations on the hole self-energy within the random-phase approximation (RPA). While the RPA does not provide a fully accurate description of $\chi(\mathbf{q},\omega)$, the qualitative effects are already apparent in this approach. In Figs. 4(a) and 4(b) the S_z and $S_\pm$ spin fluctuation contributions to the ground-state energy are shown in the presence of an added hole in momentum state $\mathbf{k}$. Two effects occur. The first is that the Pauli principle is violated by intermediate hole lines of the vacuum fluctuations which also have momentum $\mathbf{k}$, as shown in Figs. 3(a) and 3(b) for S_z and $S_\pm$ modes, respectively. This Pauli principle suppression of the vacuum fluctuations is accounted for by exchanging the lines of a vacuum fluctuation hole with that of the added hole, thereby canceling the Pauli principle violating diagram as in Figs. 3(c) and 3(d). This gives a positive contribution to Σ for electrons ($\omega > 0$) and a negative contribution for holes ($\omega < 0$). The second effect is the conventional polaron-like shift which opposes the first effect. One finds to this order that the total hole self-energy is given by

$$\Sigma(\mathbf{k},\omega) = -\frac{3}{2} iU^2 \frac{1}{N} \sum_{\mathbf{q}} \int \frac{d\nu}{2\pi} G(\mathbf{k}-\mathbf{q},\omega-\nu)\chi(\mathbf{q},\nu) , \tag{5}$$

where $\chi(\mathbf{q},\nu)$ is given in terms of the susceptibility of the noninteracting system $\chi_0(\mathbf{q},\nu)$ [Eq. (4)] by

$$\chi(\mathbf{q},\nu) = \frac{\chi_0(\mathbf{q},\nu)}{1-U\chi_0(\mathbf{q},\nu)} . \tag{6}$$

Representing $\chi(\mathbf{q},\omega)$ by a wavy line, the time ordered Feynman diagrams corresponding to these two effects are shown in Figs. 3(e) and 3(f).

For a qualitative discussion of the formation of a pseudogap we first study a simple model for $\chi(\mathbf{q},\omega)$, which contains the essential physics of the Hubbard model in the paramagnetic regime, as will be shown in Sec. IV. The model susceptibility may then be used to calculate the self-energy from Eq. (5). For simplicity we will use in (5) the propagator for the noninteracting case $G_0(\mathbf{k},\omega) = (\omega - \varepsilon_{\mathbf{k}} + i\delta\omega)^{-1}$, focusing on the paramagnetic regime with weak to intermediate coupling $U \lesssim 4t$. In the paramagnet the rotational symmetry in spin space is still preserved, and it is sufficient to consider only the longitudinal spin susceptibility for spin amplitude fluctuations.

In the adiabatic limit the spin fluctuations are slow compared to electronic frequencies and we approximate

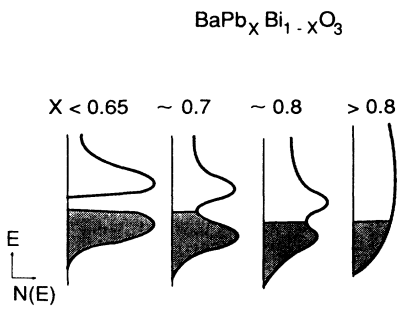

FIG. 2. Schematic representation of the change in the electronic density of states for the compositions near the metal-semiconductor transition (taken from Ref. 14).

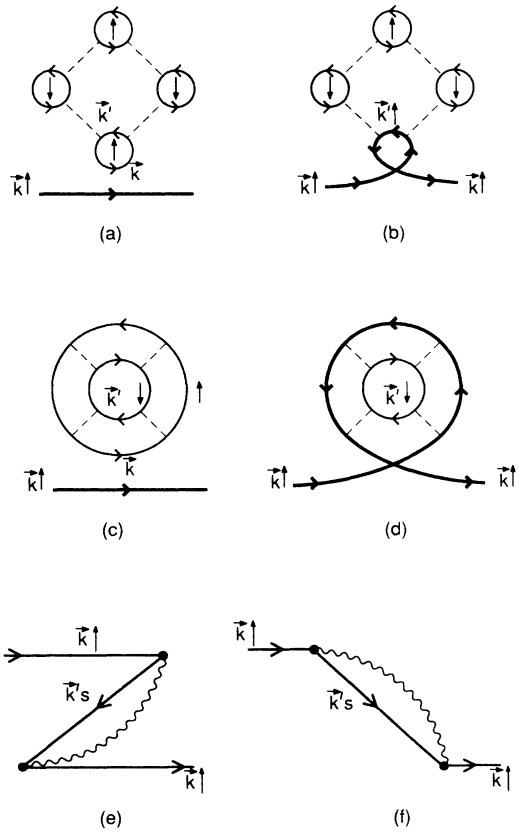

FIG. 3. Contributions to the hole self-energy $\Sigma(\mathbf{k},\omega)$ due to (a) S_z vacuum fluctuation violating the Pauli principle in the presence of the injected hole; (b) the exchange version of (a) restoring the Pauli principle; (c) and (d) the $S_\pm$ analogs of (a) and (b), (e) the "backward propagation" time ordered Feynman diagram representing (b) and (d); (f) the "forward propagation" diagram representing the polaron-like contribution to Σ. In (e) and (f) s is up or down corresponding to the spin-flip or non-spin-flip susceptibility, respectively.

the spin susceptibility by

$$\chi(\mathbf{q},\omega)=\lambda^2 2\pi i\delta(\omega)\sum_{\mathbf{Q}=(\pm\pi,\pm\pi)}\frac{\Gamma}{(\mathbf{q}-\mathbf{Q})^2+\Gamma^2}\ . \tag{7}$$

The Lorentzians are centered around the four nesting wave vectors $(\pm\pi,\pm\pi)$ their width Γ is determined by the inverse of an effective spin-spin correlation length and λ is a coupling constant. In essence, $\chi(\mathbf{q},\omega)$ represents a potential-potential correlation function $\langle V(\mathbf{r})V(\mathbf{r}')\rangle$ for a slowly fluctuating one-body interaction $V(\mathbf{r})$, whose expectation value is zero, $\langle V\rangle=0$. An analogous susceptibility has been used by Lee, Rice, and Anderson[15] to study fluctuations in a one-dimensional electron phonon system close to a Peierls instability.

The model susceptibility (7) can be easily extended to allow for finite frequency spin dynamics. For this purpose we introduce a frequency distribution $g(\omega)=(1/N_\alpha)\sum_\alpha\delta(\omega-\omega_\alpha)$ for a set of N_α characteristic frequencies ω_α, each contributing as a dispersionless propagating mode to the spin susceptibility. $\chi(\mathbf{q},\omega)$ is then given by

$$\chi(\mathbf{q},\omega)=-\int d\omega' g(\omega')\frac{2\omega'\lambda^2}{\omega^2-(\omega')^2+i\delta}\times\sum_{\mathbf{Q}=(\pm\pi,\pm\pi)}\frac{\Gamma}{(\mathbf{q}-\mathbf{Q})^2+\Gamma^2}\ . \tag{8}$$

The static Lee-Rice-Anderson–like model is recovered in the limit $g(\omega)=\lim_{\omega_0\to 0}\delta(\omega-\omega_0)$.

The frequency distribution $g(\omega)$ is assumed to be approximately independent of $\mathbf{q}$ since there are no collective modes with a well-defined dispersion $\omega(\mathbf{q})$ in the paramagnetic metal regime. We choose a simple linear (normalized) frequency distribution

$$g(\omega)=\frac{2}{\omega_0}\frac{\omega}{\omega_0}\Theta(\omega_0-\omega) \tag{9}$$

with a cutoff frequency ω_0, determining the characteristic frequency scale for spin fluctuations. However, in the adiabatic limit, when ω_0 is small compared to the SDW gap, the results of our analysis are not sensitive to the detailed form of $g(\omega)$.

With the linear frequency distribution (9) the model susceptibility (8) becomes:

$$\mathrm{Re}\chi(\mathbf{q},\omega)=\frac{4\lambda^2}{\omega_0}\left[1-\frac{\omega}{\omega_0}\frac{1}{2}\ln\left|\left|\frac{\omega+\omega_0}{\omega-\omega_0}\right|\right|\right]\phi(\mathbf{q})\ , \tag{10a}$$

$$\mathrm{Im}\chi(\mathbf{q},\omega)=\frac{2\pi\lambda^2}{\omega_0}\frac{|\omega|}{\omega_0}\Theta(\omega_0-|\omega|)\phi(\mathbf{q})\ , \tag{10b}$$

where we choose

$$\phi(\mathbf{q})=\sum_{\mathbf{Q}=(\pm\pi,\pm\pi)}\frac{\Gamma}{(\mathbf{q}-\mathbf{Q})^2+\Gamma^2}\ . \tag{11}$$

III. SELF-ENERGY

Using the model susceptibility Eq. (10) we can evaluate the real and imaginary part of the one-particle self-energy, where for simplicity we begin by replacing the full propagator G by G_0 in the RPA formula (5) and neglect vertex corrections. One finds

$$\mathrm{Re}\Sigma(\mathbf{k},\omega)=3\frac{(U\lambda)^2}{\omega_0}\frac{1}{N}\sum_{\mathbf{q}}\phi(\mathbf{q})\frac{\omega-\varepsilon_{\mathbf{k}-\mathbf{q}}}{\omega_0}\left[n_{\mathbf{k}-\mathbf{q}}\left\{\frac{\omega_0}{\omega-\varepsilon_{\mathbf{k}-\mathbf{q}}}-\ln\left|1+\frac{\omega_0}{\omega-\varepsilon_{\mathbf{k}-\mathbf{q}}}\right|\right\}-(1-n_{\mathbf{k}-\mathbf{q}})\left\{\frac{\omega_0}{\omega-\varepsilon_{\mathbf{k}-\mathbf{q}}}+\ln\left|1-\frac{\omega_0}{\omega-\varepsilon_{\mathbf{k}-\mathbf{q}}}\right|\right\}\right]\ , \tag{12a}$$

$$\mathrm{Im}\Sigma(\mathbf{k},\omega)=3\pi\frac{(U\lambda)^2}{\omega_0}\frac{1}{N}\sum_{\mathbf{q}}\phi(\mathbf{q})\frac{\omega-\varepsilon_{\mathbf{k}-\mathbf{q}}}{\omega_0}[+n_{\mathbf{k}-\mathbf{q}}\Theta(\varepsilon_{\mathbf{k}-\mathbf{q}}-\omega)\Theta(\omega_0-\varepsilon_{\mathbf{k}-\mathbf{q}}+\omega)-(1-n_{\mathbf{k}-\mathbf{q}})\Theta(\omega-\varepsilon_{\mathbf{k}+\mathbf{q}})\Theta(\omega_0-\omega+\varepsilon_{\mathbf{k}-\mathbf{q}})]\ . \tag{12b}$$

For a quantitative discussion of the self-energy (12) at $T=0$ we first consider the limit where $\phi(\mathbf{q})$ is a δ function centered at the SDW nesting wave vector $Q=(\pi,\pi)$. $\Sigma(\mathbf{q},\omega)$ is as sketched in Fig. 4 for a given momentum $\mathbf{k}$ above the Fermi surface. Due to the artificial sharp cutoff of the frequency distribution $g(\omega)$, $\mathrm{Re}\Sigma(\mathbf{k},\omega)$ has a logarithmic singularity at $-\varepsilon_{\mathbf{k}}-\omega_0$. There are three solutions for the poles of $G(\mathbf{k},\omega)=[\omega-\varepsilon_{\mathbf{k}}-\Sigma(\mathbf{k},\omega)]^{-1}$.

$$\omega-\varepsilon_{\mathbf{k}}-\mathrm{Re}\Sigma(\mathbf{k},\omega)=0\ , \tag{13}$$

which we may label as $\omega_1<\omega_2<\omega_3$. For ω_1 and ω_3 the imaginary part of the self-energy vanishes and therefore these solutions correspond to two well defined quasiparticles with infinite lifetime, indicating the presence of two quasiparticle bands. The intermediate solution ω_2, however, may be identified with the simultaneous excitation of an electron (hole) plus an incoherent cloud of spin fluctuations with momentum Q, giving rise to a finite lifetime of the order of $\omega_0/(U\lambda)^2$ as determined by the imaginary part of the self-energy $\mathrm{Im}\Sigma(\mathbf{k},\omega_2)$. This intermediate solution therefore introduces incoherent spectral weight into

$$A_{\mathbf{k}}(\omega)=\frac{1}{\pi}\frac{|\mathrm{Im}\Sigma(\mathbf{k},\omega+\mu)|}{[\omega+\mu-\varepsilon_k-\mathrm{Re}\Sigma(\mathbf{k},\omega+\mu)]^2+[\mathrm{Im}\Sigma(\mathbf{k},\omega+\mu)]^2}\ . \tag{14}$$

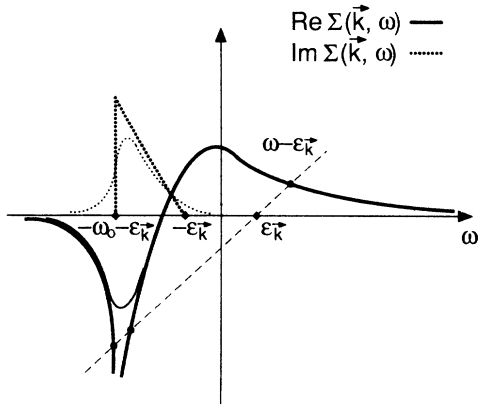

FIG. 4. Hole self-energy calculated from the model susceptibility (8) with a linear frequency distribution for spin fluctuations and in the limit $\phi(\mathbf{q})=(2\pi)^2\delta(\mathbf{q}-\mathbf{Q})$. The thin lines indicate the changes if $\phi(\mathbf{q})$ is broadened into a Lorentzian.

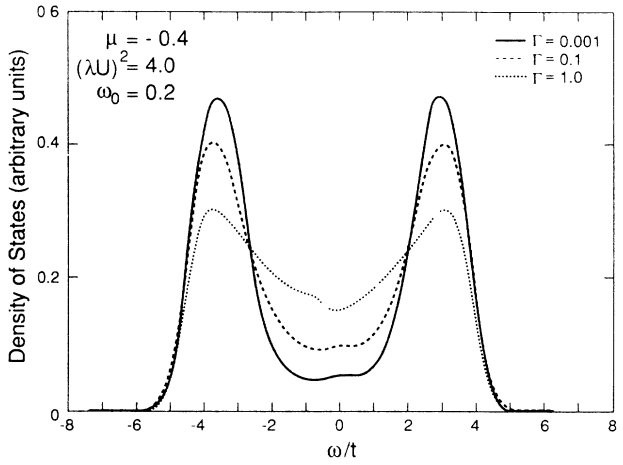

FIG. 5. Density of states as calculated from the model susceptibility for different values of Γ.

The ω_2 solution is responsible for the finite density of states in the gap leading to a pseudogap. However, we find that by using G rather than G_0 in Eq. (5) for Σ, the incoherent density of state is substantially reduced in magnitude since the decay of a quasiparticle of energy Δ leads to another particle of energy $\geq\Delta$ and a spin fluctuation of energy >0. This mechanism acts in a feedback sense, further suppressing the density of states in the gap. In the limit $\omega_0\rightarrow 0$ the lifetime of the excitations in the pseudogap, associated with the ω_2 solution, vanishes. In this limit a static SDW gap $\Delta_{\mathrm{SDW}}=2\lambda U$ exists with long-range spin order, i.e., $\phi(\mathbf{q})=(2\pi)^2\delta(\mathbf{q}-\mathbf{Q})$.

It is important to note that in the limit $\Gamma a \ll 1$ of the Lorentzian momentum distribution of the susceptibility the self-energy is strongly momentum dependent and the real part of $\Sigma(\mathbf{k},\omega)$ of quasiparticles (holes) is positive (negative) indicating that their energies are shifted away from the Fermi level compared to the energies $\varepsilon_{\mathbf{k}}$ in the absence of interactions. This shift is precisely the origin for the gap in the excitation spectrum. It also tells us that it is the suppression of vacuum fluctuations, as represented by the "backward propagation" Feynman diagram Fig. 3(e), which dominates the physics close to the metal-insulator transition. The "forward propagation" diagram shown in Fig. 3(f) for a particle injected above the Fermi surface is suppressed because close to the antiferromagnetic instability $\chi(\mathbf{q},\omega)$ predominantly transfers momentum close to the nesting wave vector $\mathbf{Q}$ to the particle. Thus, the added particles would be scattered from a state above to a state below the Fermi surface, violating the Pauli principle.

For finite increasing width Γ of the Lorentzian momentum distribution of the susceptibility the two quasiparticle peaks from ω_1 and ω_3 in $A_{\mathbf{k}}(\omega)$ broaden and develop into incoherent background contributions, while the intermediate ω_2 solution develops into the single quasiparticle of the weakly correlated paramagnetic metal. With increasing Γ the pseudogap is therefore less and less pronounced as shown by the densities of states in Fig. 5, calculated as the momentum space average of the spectral function

$$N(\omega)=\frac{1}{N}\sum_{\mathbf{k}} A_{\mathbf{k}}(\omega)\ . \tag{15}$$

In the limit where the spin-spin correlation length is reduced to a single lattice spacing, $\Gamma a=1$, the self-energy is qualitatively different as shown in Fig. 6. In this limit antiferromagnetic spin fluctuations are substantially reduced, and the self-energy is essentially momentum independent. Most importantly, the real part of the self-energy for quasiparticles (holes) cloes to the Fermi energy is now negative (positive). This indicates that the quasiparticle energies are now shifted towards the Fermi level. Since the real part of the self-energy of the quasiparticles (holes) is negative (positive) it is now the "forward propagation" diagram Fig. 3(f) representing the magnetic polaron that gives the dominant contribution to the self-energy. The smooth crossover from a Fermi liquid-like

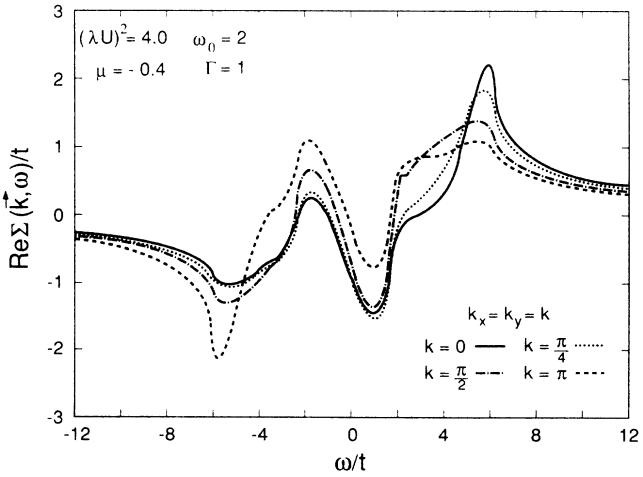

FIG. 6. Real part of the self-energy calculated from the model susceptibility for $\Gamma^{-1}=1$ (in units of the lattice spacing). Energies are measured in units of the hopping matrix element t.

metal to the pseudogap situation is therefore determined by the change in the relative importance of the "forward and backward propagation" Feynman diagrams.

Despite its simplicity the model susceptibility provides qualitative insight into how the pseudogap develops when the antiferromagnetic instability is approached. For a commensurate spin-density wave (SDW) the pseudogap will develop around the Fermi level of the undoped system. For zero damping the Fermi level falls into the pseudogap leading to insulating behavior. For finite doping concentrations the chemical potential is shifted into the large density of states regime of the broadened peaks around the edge of the pseudogap and the system will therefore behave as a Fermi liquid-like metal.

IV. NUMERICAL CALCULATION FOR THE HUBBARD MODEL

In order to show that the model susceptibility (8) indeed contains the basic physics of the single band Hubbard model in the intermediate coupling regime we calculate the self-energy (5) numerically using the random-phase-approximation (RPA) result for the susceptibility (6). For simplicity we replace the full propagator G by G_0. The frequency integral along the real axis is evaluated by deforming the integration contour into the complex frequency plane,[16] splitting up Σ into two contributions: a line integral along the purely imaginary frequency axis plus two residue contributions from the poles of G_0

$$\Sigma(\mathbf{k},\omega)=-\frac{3}{2}U^2\frac{1}{N}\sum_{\mathbf{q}}\int_{-\infty}^{\infty}\frac{d\nu}{2\pi}G_0(\mathbf{k}-\mathbf{q},\omega-i\nu)\chi(\mathbf{q},i\nu)$$
$$-\frac{3}{2}U^2\frac{1}{N}\sum_{\mathbf{q}}[(1-n_{\mathbf{k}-\mathbf{q}})\Theta(\omega-\varepsilon_{\mathbf{k}-\mathbf{q}})-n_{\mathbf{k}-\mathbf{q}}\Theta(\varepsilon_{\mathbf{k}-\mathbf{q}}-\omega)]\chi(\mathbf{q},\omega-\varepsilon_{\mathbf{k}-\mathbf{q}})\ . \tag{16}$$

Since $\chi_0(\mathbf{q},\omega)$ is an even function of frequency the integral along the imaginary axis is purely real. The imaginary part of the self-energy is therefore entirely determined by the residue contributions,

$$\mathrm{Im}\Sigma(\mathbf{k},\omega)=-\frac{3}{2}\frac{U^2}{N}\sum_{\mathbf{q}}[(1-n_{\mathbf{k}-\mathbf{q}})\Theta(\omega-\varepsilon_{\mathbf{k}-\mathbf{q}})$$
$$-n_{\mathbf{k}-\mathbf{q}}\Theta(\varepsilon_{\mathbf{k}-\mathbf{q}}-\omega)]$$
$$\times\mathrm{Im}\chi(\mathbf{q},\omega-\varepsilon_{\mathbf{k}-\mathbf{q}})\ . \tag{17}$$

The real part of the self-energy is then obtained by the Kramers-Kronig transformation:

$$\mathrm{Re}\Sigma(\mathbf{k},\omega)=P\int\frac{d\nu}{\pi}\frac{|\mathrm{Im}\Sigma(\mathbf{k},\nu)|}{\omega-\nu}\ . \tag{18}$$

Using these formulas we can straightforwardly calculate the spectral function (14) and the density of states (15). The Coulomb energy U and the chemical potential (or the particle number) are chosen to ensure that we are in the paramagnetic metal regime, not too close to the antiferromagnetic instability as determined by the Stoner criterion (3).

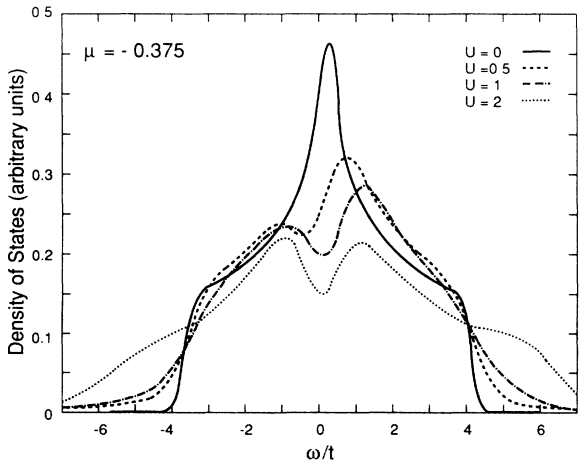

FIG. 7. Random-phase approximation density of states of the Hubbard model for different values of U.

Figure 7 shows the evolution of the zero temperature density of states with increasing U for a fixed chemical potential $\mu=-0.375t$. For this value of the chemical potential the critical Hubbard U for the Stoner instability to occur is approximately $3t$. The density of states for $U=0$ shows the usual van Hove singularity of the tight binding band in two dimensions. The momentum integrals have been performed by a coarse graining procedure on a finite lattice. The resulting density of states has then been smoothened over the discrete level spacing of the finite lattice leading to the rounding of the singularity and the band edges. As expected, with increasing U the density of states develops the pseudogap around the Fermi level. In addition, due to the increasing amplitude for spin fluctuations long tails of incoherent spectral weight appear extending far beyond the band edges. The pseudogap develops similarly for a fixed Hubbard U by increasing the chemical potential or equivalently by reducing the hole doping concentration.

V. PAIRING INTERACTION AND THE GAP EQUATION

In conventional superconductors, the exchange of one phonon between quasiparticles leads to a spin independent attractive interaction so long as the quasiparticles are within the Debye energy of the Fermi surface. However, in high-T_c materials the corresponding exchange of one antiferromagnetic spin fluctuation gives rise to a repulsion near the Fermi surface, leading to a low value of T_c and a pairing gap having d-wave symmetry.[17,18]

We have proposed an alternative pairing mechanism

for high-T_c materials based on the spin-bag approach. As demonstrated above, strong antiferromagnetic spin correlations lead to a pseudogap in the quasiparticle spectrum. The pairing attraction $V_{\mathbf{k}\mathbf{k}'}$ arises in this approach from the lowering of the system energy when two quasiparticles share the region of reduced antiferromagnetic correlations surrounding each of these excitations. The range of this attraction is of the order of the SDW coherence length ξ_{SDW}. In momentum space, this corresponds to an attraction for momentum transfer $\mathbf{q}$ smaller than ξ_{SDW}^{-1}.

In the antiferromagnetic phase, SWZ have shown[9] that the attraction between bags at small $\mathbf{q}$ is accompanied by a repulsion at large $\mathbf{q}\simeq\mathbf{Q}$, the latter being the analog of the repulsion arising from the exchange of one spin fluctuation in the paramagnetic phase. It was shown that for moderate levels of hole doping, where the Fermi surface is likely composed of several isolated pockets, the pairing gap is nonzero over the entire hole Fermi surface. However, due to the repulsive nature of $V_{\mathbf{k}\mathbf{k}'}$ for $\mathbf{k}-\mathbf{k}'$ of order $\mathbf{Q}$, the gap parameter changes sign between different pockets.

Here we investigate the pairing interaction in the paramagnetic metal phase, based on the above discussion of the pseudogap. The intent is to explore to what extent the results of the spin-bag approach join continuously as a function of doping.

Just as one can deduce contributions to the self-energy from the influence of an added hole on vacuum fluctuations (see Fig. 3) we can obtain the contributions to the effective interaction between a pair of particles by accounting for the effects on the self-energy due to the presence of the second hole. Starting with the self-energy contribution in Fig. 8(a), the presence of a second particle with the same spin and momentum as the intermediate Fermion line (not involving the bubbles) requires one to include the exchange graph Fig. 8(b) in order to restore the Pauli principle. Stretching out the lines as in Fig. 8(c), it is clear that this diagram is just the repulsive one spin fluctuation exchange process.[17] The corresponding diagram for particles of opposite spin involves an even number of bubbles. In addition, the spin flip interaction corresponding to the particle-hole ladder diagram shown in Fig. 8(d) must be added to preserve spin rotation invariance.

The effective pairing potential arising from the one spin fluctuation exchange processes is in the singlet channel given by the well-known antiparamagnon result.[19]

$$V_{\mathrm{APM}}=U+\frac{U^3\chi_0^2(\mathbf{k}'-\mathbf{k})}{1-U^2\chi_0^2(\mathbf{k}'-\mathbf{k}')}+\frac{U^2\chi_0(\mathbf{k}'-\mathbf{k})}{1-U\chi_0(\mathbf{k}'-\mathbf{k})}\ . \quad (19)$$

As mentioned above, this antiparamagnon exchange interaction is repulsive at low frequencies and gives rise to even-parity anisotropic pairing, i.e., the gap order parameter $\Delta(\mathbf{k})$ within this mechanism has d-like symmetry.[17,18] In essence, one hole sets up in its vicinity a cloud of short wavelength spin fluctuations from which the other hole scatters. The d character of the gap ensures that the holes sample the attractive regions of the potential in real space and avoid the repulsive regions.

However, the existence of the pseudogap does provide a new mechanism for an attractive spin-bag pairing potential. It arises from the exclusion principle violation shown in Fig. 9(a), where a fermion line inside one of the bubbles representing the susceptibility is equal to the momentum of the injected particle. This diagram is compensated by its exchange counterpart shown in Fig. 9(b),

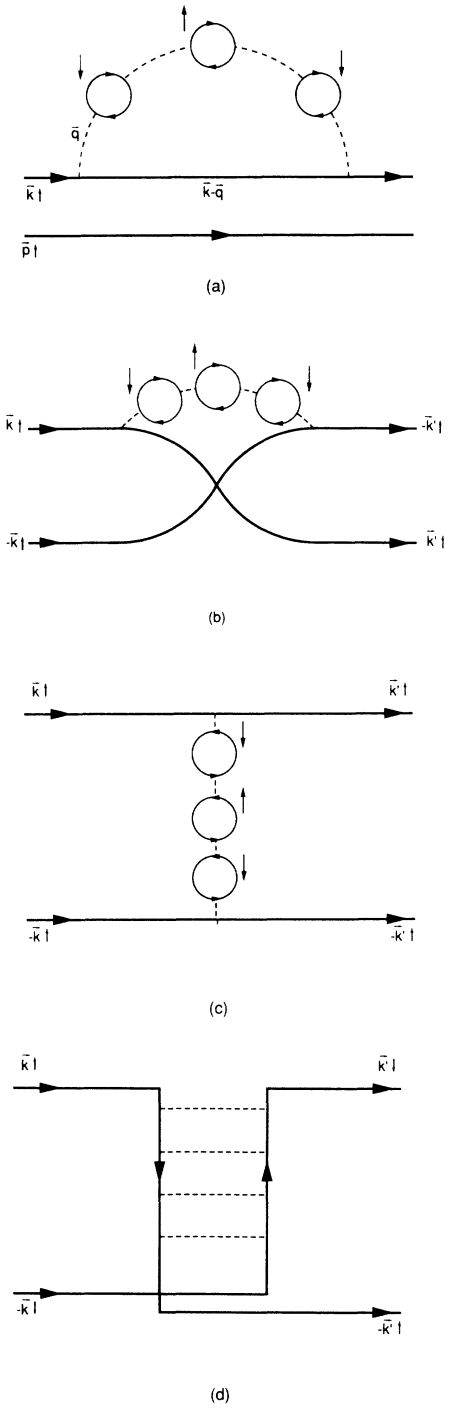

FIG. 8. (a) Self-energy diagram in the presence of a second injected particle; (b) exchange diagram restoring the Pauli principle; (c) same as in (b) with the lines stretched out; (d) particle-hole ladder diagram for the one spin-fluctuation exchange process.

or the crossed line diagram of Fig. 9(c). The fact that this diagram leads to an attraction is readily seen. As discussed above, the self-energy due to spin fluctuations is positive near the SDW instability and leads to a pseudogap. A second particle added to the system suppresses these fluctuations through the Pauli principle, reducing the phase space for electron-hole excitations and hence reducing χ. This real space reduction of susceptibility extends over a range of order ξ_{SDW} around each quasiparticle and reduces the self-energy for another particle in its vicinity, thereby giving an effective attraction. The corresponding diagram for parallel spin pairing is given by spin fluctuations lines having an odd number of bubbles.

To investigate the form and strength of the interaction between bags, we evaluate the crossed line diagram of Fig. 9(c) using the model susceptibility given in (8). Using bare propagators for the intermediate fermion lines the spin-bag pairing potential represented by this diagram is given by:

$$V^{SB}_{\mathbf{k}\mathbf{k}'}(\omega,\omega')=i\frac{1}{N}\sum_{\mathbf{q}}\int\frac{d\nu}{2\pi}G_0(\omega-\nu,\mathbf{k}-\mathbf{q})G_0(-\omega'-\nu,-\mathbf{k}'-\mathbf{q})U^2\chi(\mathbf{q},\nu)U^2\chi(\mathbf{q}+\mathbf{k}'-\mathbf{k},\nu+\omega'-\omega)\ . \tag{20}$$

Insight in the structure of this pairing potential is provided by first evaluating $V_{\mathbf{k}\mathbf{k}'}(\omega,\omega')$ with the model susceptibility (8) in the limit that there is a single spin fluctuation frequency ω_0, i.e., $g(\omega)=\delta(\omega-\omega_0)$, and the Lorentzian momentum dependence is replaced by a δ function centered at $\mathbf{Q}$, $\phi(\mathbf{q})=(2\pi)^2\delta(\mathbf{q}-\mathbf{Q})$. In this limit we find for $\omega=\omega'$:

$$V^{SB}_{\mathbf{k}\mathbf{k}'}(\omega)=-(2\pi)^2(U\lambda)^4\delta(\mathbf{k}-\mathbf{k}')\left[(1-n_{\mathbf{k}-\mathbf{Q}})^2\frac{(\omega_0-\varepsilon_{\mathbf{k}})(3\omega_0-\varepsilon_{\mathbf{k}})-\omega^2}{\omega_0(\omega_0-\omega-\varepsilon_{\mathbf{k}})^2(\omega_0+\omega-\varepsilon_{\mathbf{k}})^2}+n^2_{\mathbf{k}-\mathbf{Q}}\frac{(\omega_0+\varepsilon_{\mathbf{k}})(3\omega_0+\varepsilon_{\mathbf{k}})-\omega^2}{\omega_0(\omega_0+\omega+\varepsilon_{\mathbf{k}})^2(\omega_0-\omega+\varepsilon_{\mathbf{k}})^2}\right]\ . \tag{21}$$

Due to the δ-function approximation in the model susceptibility only momentum $\mathbf{Q}$ can be exchanged across the interaction lines giving rise to the δ-function $\delta(\mathbf{k}-\mathbf{k}')$ for vanishing net momentum transfer. The pairing potential V_{SB} is attractive for low frequencies $\omega\lesssim\omega_0$ and repulsive for high sufficiently frequencies $\omega\gg\omega_0$. This

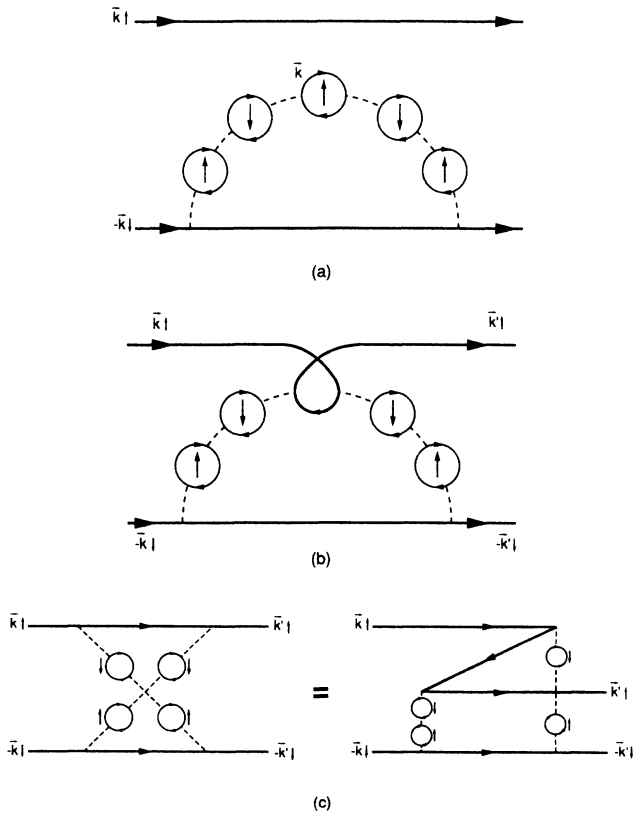

FIG. 9. Lowest-order spin-bag contribution to the pairing interaction.

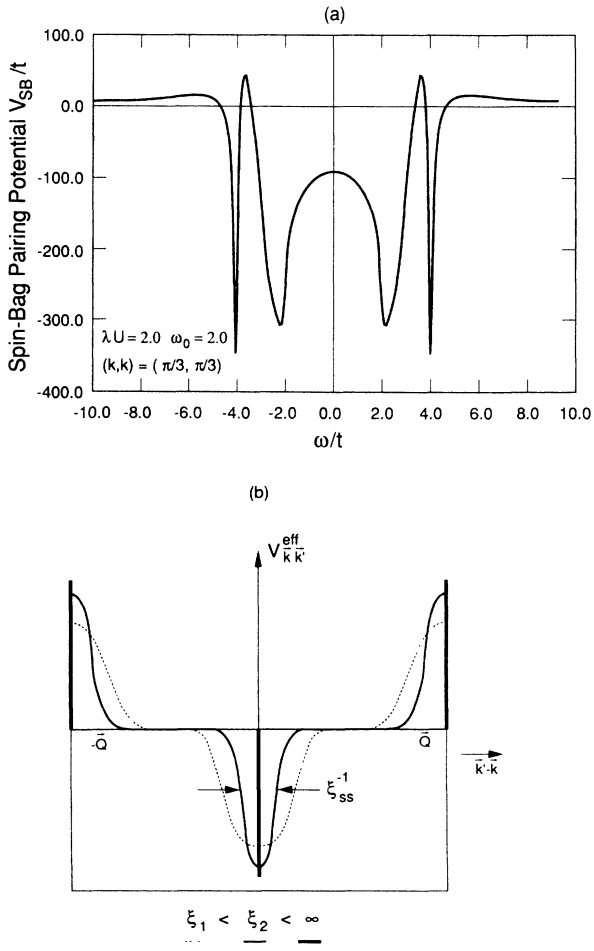

FIG. 10. (a) Frequency dependence of the spin-bag pairing potential evaluated with the model susceptibility (10) for $\phi(\mathbf{q})=(2\pi)^2\delta(\mathbf{q}-\mathbf{Q})$: (b) Momentum dependence of the effective zero-frequency pairing potential $V_{eff}(\mathbf{k},\mathbf{k}')=V_{SB}(\mathbf{k},\mathbf{k}')+V_{APM}(\mathbf{k},\mathbf{k}')$.

feature of V_{SB} is not altered by using the linear frequency distribution (8) instead of a single fluctuation frequency ω_0 [see Fig. 10(a)]. In addition, the zero-frequency limit of V_{SB} becomes strongly enhanced, diverging logarithmically at the Fermi surface precisely at half-filling.

For the case of a Lorentzian momentum distribution in the model susceptibility the spin-bag interaction broadens into a Lorentzian around $\Delta\mathbf{k}=\mathbf{k}-\mathbf{k}'\simeq 0$ with a width determined by ξ_{SDW}^{-1}. On the other hand, the contribution from the antiparamagnon exchange processes is largest for momentum transfer close to $\mathbf{Q}$ leading to an effective pairing potential $V_{eff}=V_{SB}+V_{APM}$ which is attractive for small momentum transfer and repulsive for large momentum transfer, see Fig. 10(b). This behavior of V_{eff} is independent of any special choice for the model susceptibility and merely a consequence of the Stoner enhancement for wave vectors close to $\mathbf{Q}=(\pm\pi,\pm\pi)$.

The contribution from the effective Coulomb repulsion in the charge channel still has to be added to V_{eff} giving rise to an overall upward shift. However, the effect of the Coulomb potential is weakened due to the pseudopotential scatterings far from the Fermi surface leading to a smaller probability for two electrons being within the range of the Coulomb potential.[20]

VI. SUMMARY AND CONCLUSION

We have shown how antiferromagnetic spin fluctuations depress the density of states $N(E)$ in the vicinity of the Fermi surface, leading to a pseudogap. As the system becomes antiferromagnetically ordered, the pseudogap sharpens to become the spin-density-wave (SDW) exchange gap. While it might appear that the formation of a pseudogap would require higher-order perturbation theory, the above analysis shows that the essence of the problem is already treated in the one-loop approximation for the one-particle self-energy $\Sigma(\mathbf{k},\omega)$.

The origin of the pseudogap can be understood by dividing Σ into two parts, a spin-polaron-like part Σ_{pol} and a vacuum-fluctuation part Σ_{vf}. If the spin susceptibility $\chi(\mathbf{q},\nu)$ varies smoothly with $\mathbf{q}$ as in a normal metal, Σ_{pol} dominates Σ and Fermi liquid behavior holds. However, if $\chi(\mathbf{q},\nu)$ is peaked near a wave vector $\mathbf{Q}$, as occurs when antiferromagnetic (AF) spin fluctuations are present, Σ_{vf} is strongly enhanced and Σ_{pol} is reduced. Since Σ_{vf} is due to the Pauli principle suppressing spin correlations which lower the energy in the absence of the quasiparticle, Σ_{vf} is positive for $\omega>0$, raising the energy of particle states near E_F and lowering the energy of states below E_F which accommodate holes [$\Sigma_{vf}(\mathbf{k},\omega)<0$ for $\omega<E_F$]. Therefore, the pseudogap is due to exchange suppression of vacuum fluctuations rather than a magnetopolaron effect.

Accompanying the pseudogap is a qualitative change of the one-particle spectral function $A_{\mathbf{k}}(\omega)$. While A in the Fermi liquid regime exhibits one peak at the quasiparticle energy plus incoherent continua for both particles and holes, we find that A in the pseudogap regime exhibits two main peaks, one for particles ($\omega>E_F$) and one for holes ($\omega<E_F$) for each value of $\mathbf{k}$. This behavior is analogous to a superconductor and arises from a strong smearing of $\langle n_{\mathbf{k}}\rangle$ about the Fermi surface, so that a given $\mathbf{k}$ state can accommodate both holes and electrons. Alternatively, one can view the two peaks as the precursor of the valence and conduction bands of the antiferromagnet which are folded back into the magnetic zone when long-range order sets in. We note that the two peaks come from a sharpening up of the incoherent continua of the Fermi liquid regime with the conventional quasiparticle peak being broadened and reduced to small weight, eventually vanishing as SDW order sets in.

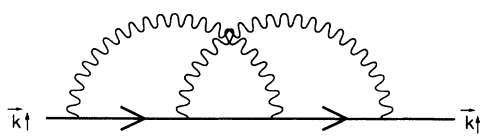

FIG. 11. Lowest-order spin-bag contribution to the self-energy. The wavy lines represent antiparamagnons.

At this level of calculation, the spectrum arises from the scattering of the injected particle by unperturbed (free) spin fluctuations present in the ground state in the absence of the added carrier. However, in next order as shown in Fig. 11, the injected particle reduces the amplitude of the fluctuations thereby reducing the size of the pseudogap over a distance of order the pseudogap coherence length $\xi_s\sim\hbar v_F/\pi\Delta_s$, where v_F is the noninteracting Fermi velocity and Δ_s is the pseudogap parameter. This combination of a hole (electron) moving with its region of reduced antiferromagnetic correlations is termed a spin bag, in essence because in strong coupling the hole is self-consistently trapped inside of the bag of reduced spin order.

We have shown that the pairing interaction $V_{\mathbf{k}\mathbf{k}'}$ between two spin bags is attractive for momentum transfer $\mathbf{q}=|\mathbf{k}-\mathbf{k}'|$ smaller than ξ_s^{-1} due to the holes sharing each other's bags. However, $V_{\mathbf{k}\mathbf{k}'}$ is repulsive for $\mathbf{q}\simeq\mathbf{Q}$, reflecting the repulsive nature of the one spin fluctuation exchange process for antiparallel spins, in contrast with the usual phonon interaction. These results are consistent with those derived by SWZ for the ordered antiferromagnet. Thus, one has a smooth evolution as the hole doping decreases from metallic to doped pseudogap and doped antiferromagnetic behavior.

While we have approximately evaluated the pairing potential in the spin-bag approach, the shape of the hole Fermi surface is also needed before one can reliably predict the detailed shape of the pairing gap parameter $\Delta_{SC}(\mathbf{k})$. If we consider hole doping at the four corners of the magnetic zone, then the repulsive nature of $V_{\mathbf{k}\mathbf{k}'}$ for $\mathbf{k}-\mathbf{k}'\simeq\mathbf{Q}$ suggests that $\Delta_{SC}(\mathbf{k})$ has d-wave-like symmetry $\Delta_{SC}(\Theta)=\Delta_0\cos(2\Theta)$ where Θ is the direction of $\mathbf{k}$ in the x-y plane. If the density of states in the pseudogap is small and the hole pockets do not overlap, the system will appear to be very different from a conventional d-wave superconductor in that the hole Fermi surface samples $\Delta_{SC}(\Theta)$ only near $\Theta_n=n\pi/2$, where $\cos(2\Theta_n)=\pm 1$ and $|\Delta_{SC}(\Theta_n)|=\Delta_0$, i.e., nodeless on the hole Fermi surface. Alternatively, if the Fermi surface is connected, a more conventional d-wave superconductor would be expected.

The above treatment can be improved in a number of directions. For example, if the self-consistent G is used to calculate Σ [Eq. (5)], a feedback effect occurs which considerably deepens the pseudogap. Vertex corrections will then have to be included in order to maintain a conserving approximation.

Based on the above treatment of spin bags in the paramagnetic phase we are presently calculating a number of experimentally observed properties of both the normal and the superconducting state. The results will be presented in a forthcoming publication.

ACKNOWLEDGMENTS

The Public Service Company of New Mexico and the U.S. Department of Energy are acknowledged for their support of the Los Alamos Advanced Studies Program in High-Temperature Superconductivity Theory. A.K. gratefully acknowledges the hospitality of the Institute for Theoretical Physics in Santa Barbara. Both of us would like to acknowledge helpful discussions with E. Abrahams, S. C. Zhang, and X. G. Wen.

---

*On leave of absence from Institut für Theoretische Physik, Universität zu Köln, Federal Republic of Germany.

†Permanent address: Department of Physics, University of California, Santa Barbara, CA 93106.

[1]Y. Tokura, H. Takagi, and S. Uchida, Nature (London) **337**, 345 (1989); A. C. W. James, S. M. Zahurak, and D. W. Murphy, *ibid.* **338**, 240 (1989).

[2]G. Shirane *et al.*, Phys. Rev. Lett. **59**, 1613 (1987); Y. Endoh *et al.*, Phys. Rev. B **37**, 7663 (1988); J. Tranquada *et al.*, Phys. Rev. Lett. **60**, 156 (1988).

[3]K. B. Lyons *et al.*, Phys. Rev. B **37**, 2353 (1988); K. B. Lyons *et al.*, Phys. Rev. Lett. **60**, 732 (1988).

[4]P. W. Anderson, Science **235**, 1196 (1987); P. W. Anderson, G. Baskaran, Z. Zou, and T. Hsu, Phys. Rev. Lett. **58**, 2790 (1987); S. A. Kivelson, D. S. Rokhsar, and J. P. Sethna, Phys. Rev. B **35**, 8865 (1987).

[5]X. G. Wen, F. Wilczek, and A. Zee, Phys. Rev. B **39**, 11413 (1989).

[6]R. B. Laughlin, Phys. Rev. Lett. **60**, 2677 (1988); Science **242**, 525 (1988).

[7]S. Schmitt-Rink, C. M. Varma, and A. E. Ruckenstein, Phys. Rev. Lett. **60**, 2793 (1988); C. L. Kane, P. A. Lee, and N. Read, Phys. Rev. B **39**, 6880 (1989); B. I. Shraiman and E. D. Siggia, Phys. Rev. Lett. **60**, 740 (1988); *ibid.* **61**, 467 (1988); R. Shankar, *ibid.* **63**, 203 (1989); S. A. Trugman (unpublished); Y. Hasegawa and D. Poilblanc (unpublished); E. Dagotto, A. Moreo, R. Joynt, S. Bacci, and E. Gagliano (unpublished).

[8]The existence of spin bags and the physical mechanism by which they produce an attractive pairing interaction in the paramagnetic metal phase was discussed by J. R. Schrieffer (unpublished).

[9]J. R. Schrieffer, X. G. Wen, and S. C. Zhang, Phys. Rev. Lett. **60**, 944 (1988); Phys. Rev. B **39**, 11663 (1989).

[10]A. B. Harris and R. V. Lange, Phys. Rev. **157**, 295 (1967).

[11]J. D. Reger and A. P. Young, Phys. Rev. B **37**, 5978 (1988).

[12]J. E. Hirsch and D. J. Scalapino, Phys. Rev. Lett. **56**, 2732 (1986).

[13]Y. Hasegawa and H. Fukuyama, Jpn. J. Appl. Phys. **26**, L322 (1987); H. J. Schulz (unpublished).

[14]K. Kitazawa, S. Uchida, and S. Tanaka, Physica (Utrecht) **135B**, 505 (1985); S. Uchida, K. Kitazawa, and S. Tanaka, Phase Transitions **8**, 95 (1987).

[15]P. A. Lee, T. M. Rice, and P. W. Anderson, Phys. Rev. Lett. **31**, 462 (1973).

[16]J. P. Blaizot and B. L. Friman, Nucl. Phys. **A372**, 69 (1981).

[17]D. J. Scalapino, E. Loh, Jr., and J. E. Hirsch, Phys. Rev. B **34**, 8190 (1966); D. J. Scalapino and E. Loh, Jr., *ibid.* **35**, 6694 (1987); K. Miyake, S. Schmitt-Rink, and C. M. Varma, *ibid.* **34**, 6554 (1986).

[18]J. E. Hirsch, Phys. Rev. Lett. **54**, 1317 (1985).

[19]S. Nakajima, Prog. Theor. Phys. Jpn. **50**, 1101 (1973); P. W. Anderson and W. F. Brinkman, Phys. Rev. Lett. **30**, 1108 (1979); D. Fay and J. Appel, Phys. Rev. B **22**, 3173 (1980).

[20]N. N. Bogoliubov, Nuovo Cimento **7**, 6 (1958); P. Morel and P. W. Anderson, Phys. Rev. **125**, 1263 (1962); J. Kanamori, Prog. Theor. Phys. **30**, 275 (1963).

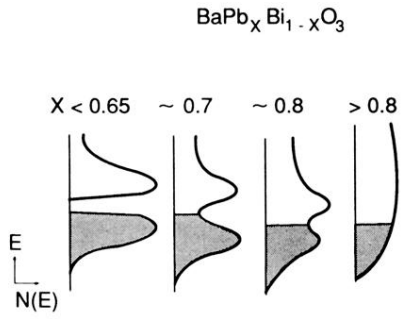

FIG. 2. Schematic representation of the change in the electronic density of states for the compositions near the metal-semiconductor transition (taken from Ref. 14).